Est. 1984

ORIENTAL JOURNAL OF CHEMISTRY
An International Open Access, Peer Reviewed Research Journal

www.orientjchem.org

ISSN: 0970-020 X
CODEN: OJCHEG
2022, Vol. 38, No.(6):
Pg. 1489-1497

Electroless Ni-W-P Alloy Deposition on Mildsteel using Lawsone as Complexing Agent

H. ASIA THABASSOOM[1] and J. FELICITA FLORENCE[2]

Research Department of Chemistry, Holy Cross College (Autonomous),
Affiliated to Bharathidasan University, Tiruchirappalli-620002, India.
*Corresponding author E-mail: asia.shahbir@gmail.com

http://dx.doi.org/10.13005/ojc/380622

(Received: September 29, 2022; Accepted: December 17, 2022)

ABSTRACT

Electroless coatings have been used in many industries now days due to their good properties, such as corrosion and wear resistance, hardness and uniform thickness. Nickel sulphate and Sodium tungstate are used as Nickel and tungsten sources respectively, Sodium hypophosphite is used as reducing agent. The effect of Lawsone isolated from Lawsonia inermis Linn leaf extract and found that complexing agent Sodium citrate is replaced by Lawsone which enhances plating properties. In order to characterise Ni-W-P surfaces, SEM, EDAX and XRD methods are used. We looked at the Ni-W-P corrosion resistance behaviour as well as electrochemical techniques such potentiodynamic polarisation curve and electrochemical impedance spectroscopy. Metal that is electrolessly deposited has good corrosion resistance.

Keywords: *Lawsoniainermis Linn* leaf, SEM, EDAX, XRD and polarization studies.

INTRODUCTION

Electroless plating, sometimes referred to as chemical plating or auto-catalytic plating, is a non-galvanic plating method that incorporates numerous continuous chemical processes in an aqueous solution without the usage of external electrical power. A reducing agent, usually sodium hypophosphite, releases hydrogen during the process, which is then oxidised to produce a negative charge on the part's surface[1-2]. The most popular electroless plating technique is electroless nickel plating. The driving force behind the reduction of nickel metal ions and their deposition in the Electroless plating process is a chemical reducing agent in solution. Because of this, the thickness of electroless deposits is fairly consistent across the part's size and shape.The mechanical characteristics were further enhanced by the Ni-P-W alloy coating, which combined solution and precipitation hardening of Ni-P. Due to their unique physical, chemical, and mechanical characteristics, electroless coatings have gained widespread use in surface engineering and metal finishing applications in sectors like the automotive, petrochemical, electronics, maritime, and mining industries[3-4].

Lawsonia inermis, a member of the Lythraceae family with natural distribution in North Africa and Southwest Asia, is widely grown as an

ornamental and dye plant in India. Henna is known by another name for it, Lawsonia inermis Linn. A decoction gargled could ease a sore throat. There have been assertions made about the analgesic, anti-inflammatory, hepatoprotective, antimitotic, immunomodulatory, antiviral, antibacterial, and antifungal properties of these compounds.

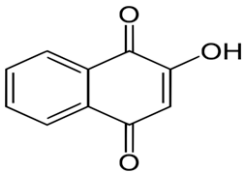

Due to its excellent dye property, Lawsoniainermis (henna), which has been used as a skin and hair colour for more than 5000 years, inhibitive action of henna extract (Lawsonia inermis) where its main constituents (Lawsone, Gallic acid, a-D-Glucose and tannic acid) on corrosion of mild steel was investigated through electrochemical techniques and surface analysis[5-6]. 2-hydroxy-1, 4-naphthoquinone, chemical formula $C_{10}H_6O_3$ has significant anti-inflammatory, anticancer, antioxidant, and anticorrosion properties. Lawsonia inermis has high corrosion-inhibitory properties. The study involves the effect of Lawsone to extract the inhibitor which was used for the immersion test where Lawsonia Inermis was extracted by ethanol.

EXPERIMENTAL

Mild steel serves as the substrate for Ni-P electroless plating (12 cm x 6 cm x 0.1 mm). The substrates are completely rinsed after being degreased with acetone, cleaned alkalinely with sodium hydroxide, then cleaned acidically with Conc. HCl. After drying with a gentle cloth, apply wax. The following substances are utilised in the electroless bath: nickel sulphate (30 g/L), sodium hypophosphite (14 g/L), sodium citrate (30 g/L), ammonium sulphate (10 g/L), and sodium tungstate (10 g/L) as nickel ion sources, complexing agents, and reducing agents, respectively[7-9]. On mild steel specimens, electroless plating takes two and a half hours. The rate of deposition is calculated using the formula below.

$$\text{Rate of deposition} = \frac{\text{Weight of the deposit X } 10^4 \text{ X } 60}{\text{Area X Density X time}} \quad (1)$$

Lawsone is isolated from Lawsoniainermis Linn leaf extract using Tommasi's procedure.

Characterization of plating

The elemental structure of the deposits is verified by energy dispersive X-ray analysis and SEM, which are both employed to study the nanocrystalline Ni-P coatings on mild steel. (EDAX). The crystalline structure and grain size of the Ni-P deposit coating were determined using a Philips X'pert X-ray diffractometer with CuK radiation. The behaviour of corrosion is evaluated using potentiodynamic polarisation curves.

RESULTS AND DISCUSSION

Optimization of Ni-W-P Electroless plating:

Lawsone, 2-hydroxy-1, 4-Napthoquinone, a red dye derived from Lawsoniainermis Linn's leaves, is crucial for enhancing the surface qualities of mild steel that has been electroplated. In this study, the effects of Lawsone as addition agent(LAA) and complexing agent (LCA) in Ni-W-P electroless deposition are being investigated. The objective of the present work is to create electroless Ni-W-P deposited on mild steel using reducing agents sodium hypophosphite and sodium tungstate, complexing agents sodium citrate, and accelerating agents ammonium sulphate. Henna leaves contain the colourant Lawsone, which can be isolated as yellow and orange crystals. By adding 1-6 mL of Lawsone to the basic bath composition for electroless Ni-W-P deposition, the effect of the addition agent is examined. Deposition is accelerated by adding 4 mL of Lawsone[10-13]. The visual brightness is caused by the addition agent's increased deposition rate. 4 mL is the recommended concentration for Lawsone. In electroplating, nickel sulphate is a highly soluble blue-green salt and is employed as a source of the Ni^{2+} ion.In electroplating and as a chemical intermediary in the manufacture of other nickel compounds, nickel sulphate is utilised. By utilising 5 g for each plating and holding the addition agent, Lawsone, at 4 mL, the concentration of nickel sulphate hepta hydrate is adjusted from 1g/L to 20 g/L. The ideal concentration of nickel sulphate hepta hydrate is 20 g/L since this concentration yields the highest deposition rate.

Table 1: The Effect of Lawsone

Lawsone(2-Hydroxy-1,4 Naphthoquinone)	Rate of deposition(μ/h)
1 mL	3.8
2 mL	5.7
3 mL	10.25
4 mL	12.6
5 mL	11.8
6 mL	9.4
7 mL	7.6

Table 2: The Effect of $NiSO_4.7H_2O$

$NiSO_4.7H_2O$ (g/L)	Rate of deposition (μ/h)
5	3.0
10	5.3
15	9.2
20	10.0
25	7.5
30	4.6
35	2.8

Sodium hypophosphite has the ability to convert metal ions back into base metal. The primary industrial use, electroless nickel plating (Ni-P), is built on top of this. It changes nickel ions in solution to metallic nickel on both metal and plastic substrates. Table 3 shows that the rate of electroless nickel deposition increases as sodium hypophosphite concentration rises up to 10 g/L. As sodium hypophosphite monohydrate concentration rises, so does the rate of deposition. The rate of deposition rises to 12.3/h when the $NaH_2PO_2.H_2O$ concentration reaches 10 g/L. Therefore, it is thought that this sodium hypophosphite monohydrate concentration of 10g/L is ideal. The deposit's phosphorous content rises as H_2PO_2-concentration rises[14-16]. The inorganic compound sodium tungstate has the formula Na_2WO_4. The sodium salt of tungsten acid is this yellowish, water-soluble solid. It can be utilised as a source of tungsten in chemical synthesis. It is a phase in turning tungsten ores into metal. As sodium tungstate concentration rises from 1 g to 6 g/L, the rate of deposition accelerates until it reaches a maximum of 3 g/L. This concentration is seen as optimum as a result.

Sodium citrate is utilised as a complexing agent during the deposition of nickel. According to Table 6, 20 g/L of sodium citrate results in the highest nickel deposition rate. When the sodium citrate concentration is increased to 20 g/L, the deposition rates are decreased. Higher sodium citrate concentrations produce a drop in the concentration of free ions, which causes metal ions to take on the characteristics of complex or chelated nickel ions and slow down deposition. The concentration of ammonium sulphate, which is found to be at its greatest at 5 g/L, causes an increase in the rate of deposition. The bath containing 5 g/L of ammonium sulphate is therefore chosen as having the optimal concentration for Ni-W-P electroless deposition.

Table 3: The Effect of sodium hypophosphite

Sodium hypophosphite monohydrate ($NaH_2po_2.H_2o$) g/L	Rate of deposition (μ/h)
2	2.5
4	4.7
6	5.9
8	8.3
10	10.3
12	8.8

Table 4: The Effect of Sodium Tungstate

Sodium tungstate g/L	Rate of deposition (μ/h)
1	1.2
2	4.1
3	6.6
4	3.9
5	2.8
6	1.3

Table 5: The Effect of Sodium citrate

Sodium Citrate Monobasic Hydrate ($Na_3C_6H_5O_7.H_2O$) g/L	Rate of deposition (μ/h)
5	6.23
10	7.51
15	9.61
20	11.6
25	8.8
30	6.3
35	5.5

Table 6: The Effect of Ammonium Sulphate

Effect of NH_4SO_4 g/L	Rate of Deposition (μ/h)
1	11.72
2	12.6
3	16.42
4	18.37
5	21.9
6	17.98
7	12.05

Table 7: The Effect of temperature

Effect of Temperature (°C)	Rate of Deposition (μ/h)
30^o	1.32
40^o	3.9
50^o	6.21
60^o	12.44
70^o	8.26
80^o	6.7

Table 8: The Effect of pH

Effect of pH	Rate of Deposition (µ/h)
3	2.82
4	4.9
5	7.21
6	9.44
7	8.26
8	7.7

Table 9: The Effect of plating time

Effect of Plating Time (min)	Rate of Deposition (µ/h)
30	2.23
60	6.66
90	10.80
120	14.67
150	17.5
180	11.45

The rate of electroless nickel deposition rapidly increases between 30 and 90° Celsius. The rate of deposition is almost twice as quick at 60°C. The coating, however, seems dull at high temperatures. Therefore, the ideal temperature for excellent electroless nickel is 60°C. Temperature has a considerable effect on the electrolessbath because it produces the energy needed for the chemical bonding that results from metal oxidation[17-20]. The table shows that the rate of deposition increases with temperature and pH, peaking at 60°C at pH 6. The rate of electroless nickel deposition increases linearly from 30 to 150 min, as shown in Table 9. The table shows that as plating time is increased up to 150 min, the rate of deposition increases.This is regarded as the ideal plating time for Ni-P-W electroless deposition when Lawsone is present[21-23]. Additionally, for industrial applications, lengthening the deposition time is economically unfavourable.

Optimized Bath Composition

By adjusting the various bath components when the additive Lawsone is present, the bath composition is optimised for Ni-P electroless deposition.

Table 10: Optimized Bath composition on Electroless Ni-W-P deposition

Nickel sulphate hepta hydrate	20 g/L
Sodium hypophosphite	10 g/L
Sodium tungstate	3 g/L
Ammonium sulphate	5 g/L
Sodium citrate	20 g/L
Temperature	60°C
pH	6
Lawsone	4 mL

Lawsone as complexing agent

To determine the role of lawsone in this Ni-W-P scenario Lawsone replaces bath components such as sodium hypophosphite, ammonium sulphate, and sodium citrate in the electroless deposition process. Finally, the rate of depositon and plate surface properties are increased by removing sodium citrate with 4 mL of Lawsone. This demonstrates that Lawsone can function as a complexing agent. Table 11 shows the optimised bath composition with Lawsone as the complexing agent.

Table 11: Optimized Bath-Lawsone as Complexing Agent

Nickel sulphate hepta hydrate	20 g/L
Sodium hypophosphite	10 g/L
Sodium tungstate	3 g/L
Ammonium sulphate	5 g/L
Temperaturea	60°C
pH	6
Lawsone	4 mL

Surface morphology

SEM analysis

SEM is used to evaluate the surface of the electroless Ni-W-P deposited mild steel. Figures shows that the electroless Ni-W-P that the BB has deposited on mild steel contains porous spherical nodules with little grain inside of them (a). According to figures, the grains in the LAA exhibit are not all the same size and have a clear nodular structure (b). Figure shows the Transmission electron microscopy pictures of LCA, which are homogeneous, compact, brilliant, and smooth without any evident flaws like peeling, pitting, cracking, bubbling, delamination, or nodulation. They also feature a well spaced cellular structure with matte texture (c).

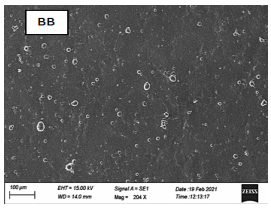

Fig.1a. (BB)

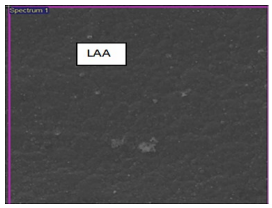

Fig.1b. (LAA)

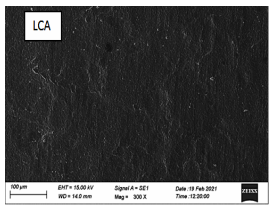

Fig. 1c. (LCA)

EDAX analysis

EDAX examination:Under BB, LAA, and LCA conditions, this is the element % used in electroless Ni-W-P deposition. The percentage of the elements as well as the EDAX spectra of electroless Ni-W-P deposited on mild steel from the BB, LA, and LC are shown in the figure. In BB electroless Ni-W-P deposited mild steel, the weight percentages of nickel, tungsten, phosphorus, and oxygen are 75.67%, 6.17%, 15.98%, and 2.17%, respectively. It is established that the weight percentages of nickel, phosphorus, and tungsten in the LA bath are 83.49%, 12.51% and 4.23%, respectively. The weight percentages of nickel, tungsten, phosphorous, and oxygen in electroless Ni-W-P deposited mild steel from LC are 79.79%, 2.26%, 7.36%, 1.67%, and 3.67%, respectively.The coating has a medium phosphorous concentration since the proportion of phosphorous ranges from 2 to 12%. Due to the large proportion of phosphorus, it belongs to the group of coatings with a high phosphorus content. Higher Phosphorus content coatings offer good corrosion resistance in the as-deposited state, according to prior research[24-28].

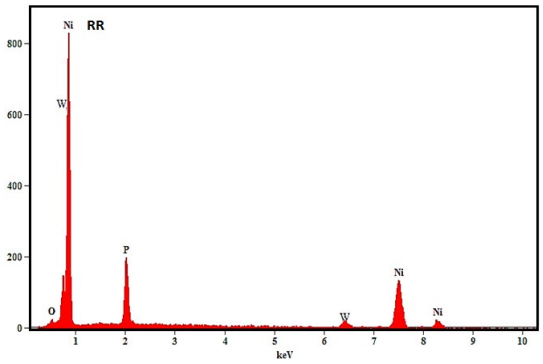

Fig. 2a. (BB)

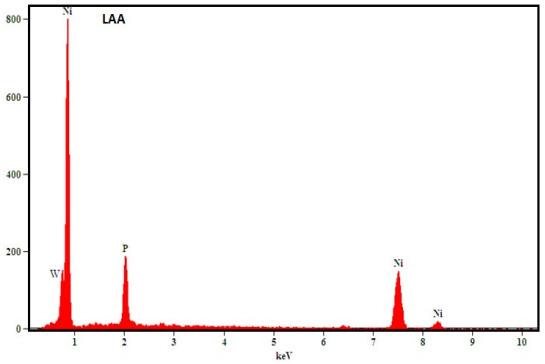

Fig. 2b. (LAA)

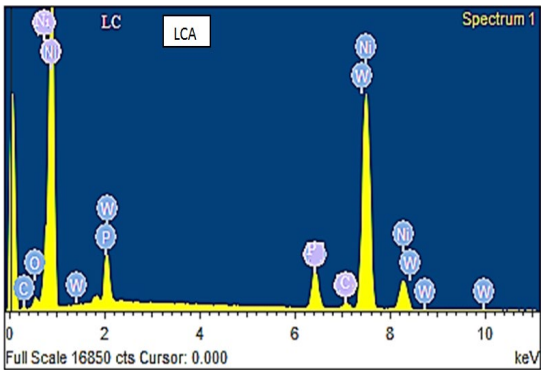

Fig. 2c.(LCA)

Table 12: Edax analysis

Bath	Nickel	Tungsten	Phosphorous
BB	75.67	6.17	15.98
LAA	83.49	4.23	12.71
LCA	79.79	2.26	7.36

X-ray diffraction studies

The Electroless Ni-W-P reserves' XRD patterns are displayed as, with one notable peak with a Nickel intensity showing at roughly 2θ=45°, demonstrating the deposits' Crystalline nature. The deposits amplitude sharply increased, maybe indicating that some Ni-W-P deposits crystallised. In the electroless Ni-W-P deposit, the broad peak is obtained from the diffraction of amorphous or nanocrystalline phase, and the highest absorbance is obtained from the (1 1 1) diffraction of nanocrystalline Ni[29-31]. Despite the fact that the phosphorus concentration is almost equal, this assumes that the structure of the Ni-W-P deposit is separate. According to, the sharp peaks of BB are roughly 45°, 65°, 82°, 98°, and

116°, while the textures of FCC have (111), (211), (221), and (222). (a). The LAA appears to be 45°, 52°, 65°, 76°, and 82° as shown in the Figure, with FCC structures of (111), (200), (211), and (200), respectively (221). (b). Figure illustrates the usage of FCC textures (111), (211), and (221) at LC intensities of 45°, 65°, and 82°. (c). The X-ray diffraction analysis of an electroless Ni-W-P deposited thin layer of mild steel possessed strong peaks when compared to the peaks obtained from the BB, LA, and LC[29-31]. The production of crystalline nickel on mild steel is indicated by the strong peaks. It is predicted that the grain size and FWHM of BB will be 60.64 nm and 0.2°, compared to LA's 62.015 nm and 0.26° and 61.83 nm and 0.21°, respectively. The coating of LA has an amorphous structure. Scherer's equation is used to determine size.

$$D=B\lambda/\beta Cos\theta \quad (2)$$

Where D is the average crystallite size of the phase being studied, B is the Scherer constant (0.89), is the X-ray beam's wavelength, FWHM (full width at half maximum) is the diffraction, and is the Bragg's angle.

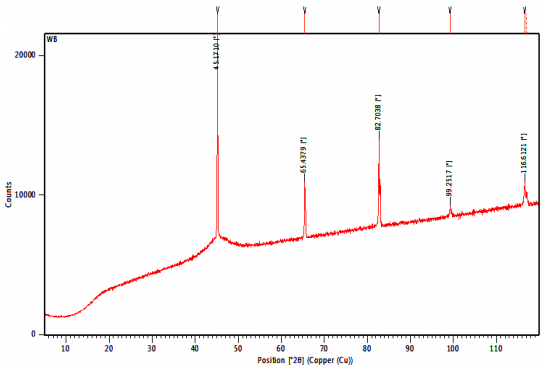

Fig. 3a. (BB)

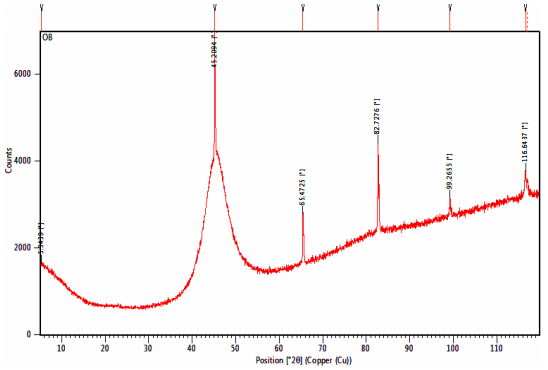

Fig. 3b. (LAA)

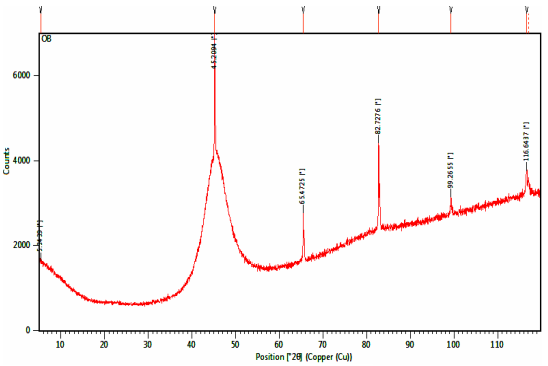

Fig. 3c. (LCA)

Potentiodynamic polarization measurements for corrosion resistance of coatings

Figures depict the potentiodynamic curves of Ni-W-P deposits in a 3.5% NaCl aqueous solution. The deposits examined were BB, LAA, and LCA deposits that were as-plated and had a range of structural compositions. The corrosion potential E_{corr} and anodic current density I_{corr} can be calculated by intersecting the cathodic and anodic Tafel curves, which are extrapolated from the cathodic and anodic potentiodynamicpolarisation curves. As seen in the Tables 14, the ternary Ni-W-P deposits of various configurations have a similar corrosion tendency.Comparing the as-plated Ni nanocrystalline deposit to its amorphous, mix-structure, and annealed equivalents, it has the lowest E_{corr} and the highest I_{corr}, making it

potentially the least corrosion resistant. The as-plated BB mix-structure deposit has a much lower icorr than the as-plated LA nanocrystalline deposit, although having a higher icorr than the LC amorphous deposit. This finding confirms the XRD study that the as-plated deposit LC structure is a mixture of nanocrystalline and amorphous phases.The Ni-W-P deposition is relatively corrosion-resistant in 3.5% NaCl. In order to demonstrate corrosion resistance, phosphorus caused the corrosion potential to shift to the right by lowering the corrosion current density. The R_{ct} is determined at a low frequency in contrast to the solution resistance, which is determined at a high frequency. This plot has the advantage of displaying information for all of the recorded frequencies as well as a wide range of impedance values.

Table 13: Tafel polarization

Bath	E_{corr}	I_{corr}	βc	βa	R_{ct}	R_p	C_{dl}
BB	-491.812mV	57.135 µA	10.859V	86.161mV	1.76	8.7042	$1.6x10^{-3}$
LAA	-751.745mV	130.947 µA	391.042mV	56.634mV	6.87	8.6872	$1.03x10^{-2}$
LCA	-764.417 mV	241.111 µA	136.255 mV	477.606 mV	10.974	7.1932	$3.17x10^{-3}$

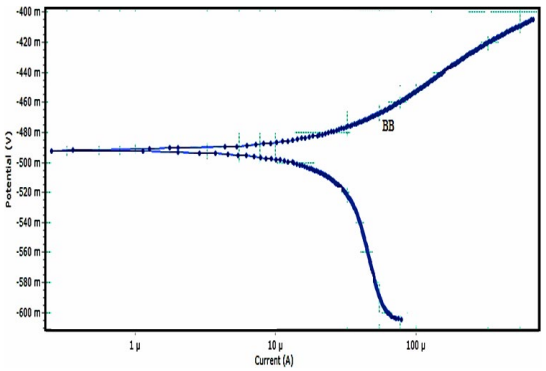

Fig. 4a. (BB)

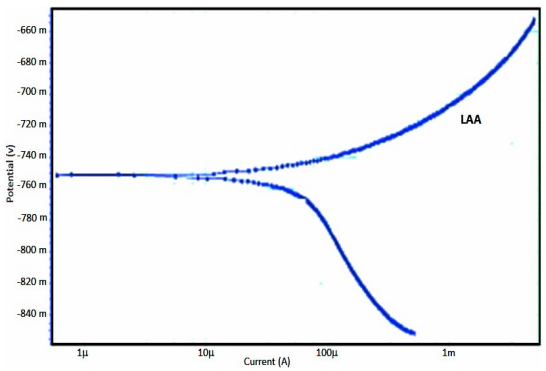

Fig. 4b. (LAA)

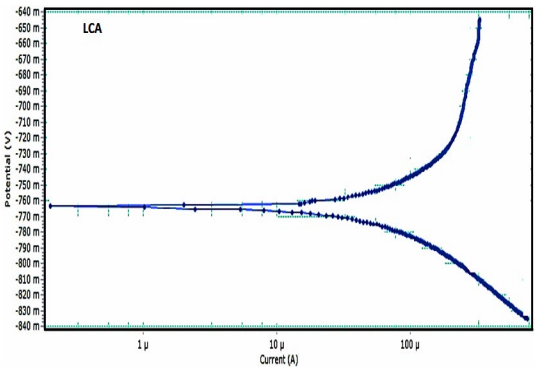

Fig. 4c. (LCA)

Electrochemical impedance spectroscopy (EIS) studies

Following electroless Ni-W-P deposition in a 3.5% NaCl solution, the observed impedance spectrum of the mild steel substrate is shown in Figure. Metallic coatings can be distinguished by the formation of a single semicircle or a semicircle followed by a low frequency loop. The Nyquist plots have curves that are identical in shape but have vastly varied sizes. When an additive is present, the semicircle of the Nyquist plots is depressed. The diameter of the impedance plot increased with the inclusion of Lawsone. The semicircle dip is frequently attributed to surface roughness, solid surface inhomogeneity, and inhibitor adsorption on the metal surface[32-33].

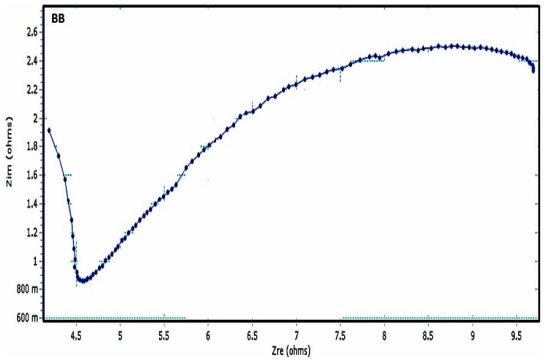

Fig. 5a. (BB)

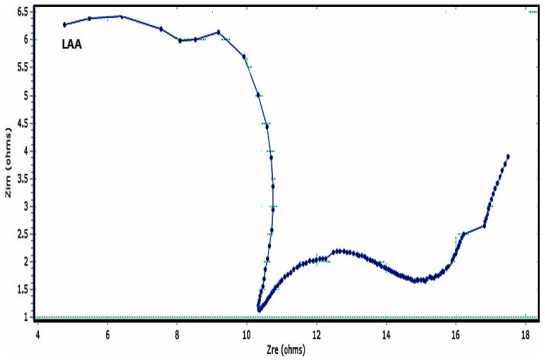

Fig. 5b. (LAA)

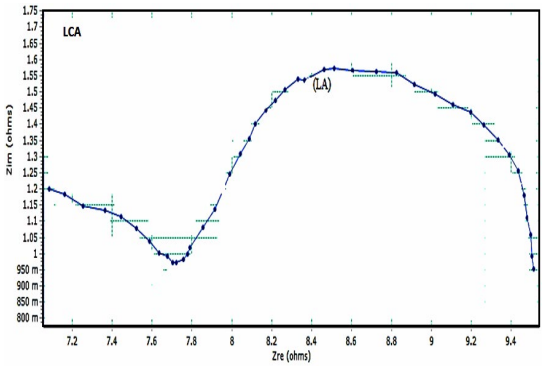

Fig. 5c. (LCA)

CONCLUSION

This is the first report on electroless Ni-W-P deposition with grain sizes less than 100nm from an alkaline bath. The results of XRD, EDAX and SEM revealed their structure, composition, and morphology. We believe that this method will pave the way for the deposition of metallic structures on mild steel substrates with desired properties.Corrosion tests show that electroless Ni-W-P coatings deposited in all conditions significantly improve mild steel corrosion resistance. Green synthesised Ni-W-P deposits are widely used in the automotive and aerospace industries.

ACKNOWLEDGEMENT

I thank our institute holy cross college (Autonomous), Trichy for providing labarotory facilities.

REFERENCES

1. Loto, C.A., *Electroless Nickel plating, Springer Science.*, **2016**, *8*, 177-186.
2. Brenner, Abner.; Riddell, Grace E, *Journal of Research of the National Bureau of Standards.*, **2018**, *37*, 31–34.
3. Agarwala R.C, Vijaya Agarwala, *Springer.*, **2003**, *28*, 475-493.
4. Latha, N.; Raj, V.; Selvam, M.; Manisankar, P.; *Int. J. Chem. Sciences.*, **2012**, *10*(1), 479-489.
5. Ashnagarand, A.; Shiri, A.; *International J. of ChemTech Research.*, **2011**, *3*, 1941-1944.
6. Felicita Florence, J.; Susai Rajendran.; SrinivasanK. N.; *International Journal of Innovative Science, Engineering & Technology.*, **2015**, *2*, 505-516.
7. K. G. Keong.; W. Sha.; S. Malinov., *J of Non Crystalline Solids.*, **2003**, *324*, 230-241.
8. Abdel salam.; Hamdy, Shoeib. M. A.; Hady. H.; Abdelsalam, O. F.; *Journal of Appl. Electrochem.*, **2008.,** *38*, 385-394.
9. Uma Rani.; Anand kumar Sharma.; Minu. C.; Poornima. G.; *J of Applied Electrochemistry.*, **2010**, *40*(2), 333-339.
10. Ayoub, I. E.; Ibrahim. I. S.; Dakroury. A. El.; *Journal of Radiation Research* and Applied Sciences., **2009**, 467-476.

11. Valova, E.; Georgieva, J.; Armyanov, S.; Dille, J.; Kubova, O.; Delplancke-Ogle M. P.; *Surface and Coatings Technology*., **2010**., *204*, 2775-2781.
12. Yuan. X.; Xie, T.; Wu. G.; Lin. Y.; Meng G.; Zhang L.; Physical E: *Low-dimensional System and Nanostructures*., **2004**, *23*, 75-80.
13. Tien S. K.; Duhand. T. J.; Chen. Y. L.; *Surface and Coatings Technology*., **2004**, *177*, 532-536,
14. Pang, J.; Li. Q.; Wang. W.; Xuand. X.; Zhai. J.; *Surface and Coatings Technology*., **2011**, *205*, 4237-4242.
15. Chivavibul, P.; Enoki, M.; Konda S.; Inada, Y.; Tomizawa T.; Toda. A., *Journal of Magnetism and Magnetic Materials*., **2011**, *323*, 306-310,
16. Krishnaveni, K.; Sankara Narayanan.T.; Seshadri.T.; *Surface and Coatings Technology*., **2005**, *190*(1), 115-121.
17. Ger, M. D.; Hou K. G.; Hwang. B. G.; *Materials Chemistry and Physics*., **2004**, *87*, 102-108.
18. Mafiand I. R.; Dehghanian C.; *Applied Surface Science*., **2011**, *257*, 8653-8658.
19. Chen, W.; Gao. W.; He. Y.; *Surface and Coatings Technology*., **2010**, *204*, 2493-2498.
20. Huang, Y.; Zeng, X.; Annergren, I.; Liu. F.; *Surface and Coatings Technology*., **2003**, *167*, 207-211.
21. Wang, Y. W.; Tu, J.; Chen, W.; Wang, Y.; Liu. X.; Cheng. D.; Zhang. Z., *Composite Coatings*., **2003**, *254*, 1289-1293.
22. Seidel, R.; Liebau, M.; Duesberg, G. M.; Kreupl, F.; Uuger, E.; Graham, A. P.; Hoenlein W.; Pompe, W.; *Nano Letters*., **2003**, *3*, 965-968.
23. Abdel Hamid, Z.; Ghanem W. A.; Abo El Enin.; A. L.; *Surface and Interface Analysis*., **2005**, *37*, 792–796.
24. Li-ping, W. U.; Zhao Jing-jing.; XIE Yong-ping, and Yang Zhong-dong.; *Trans. Nonferrous. Metals. Soc*., **2010**, *20*, 630-637.
25. Santhosh Yadav.; Anil Kumar and Ashok Kumar., *International Journal of Pharmaceutical and Chemical Sciences*., **2013**, *2*(2).
26. Kari Basavaraja, D.; Skanda, M. G., soumya, C.; Ramesh, V., *International Scholarly and Scientific Research and Innovation*., **2017**, *11*(2).
27. Suman Kalyan Das.; Prasanta Sahoo., *Research gate*., **2010**, *23*(2), 81-97.
28. Zhao. G. L.; Zou. Y.; Hao. Y. L.; Zou. Z. L.; *Archives of Metallurgy and Materials*., **2015**, *20*(2).
29. Song. Y. W.; Shan D. Y.; Han, E. H.; *Electrochemical Acta*., **2009**, 2009-2015.
30. Naiming Miao.; Jinjin Jiang.; Wang ping. W. U.; *Journal of Nanomaterials*., **2018**, *20*.
31. Matías Monroy-Cárdenas.; Oscar Forero-Doria.; Ramiro Araya-Maturana Maximiliano Martínez-Cifuentes.; *Materials*., **2021**, *14*, 5587.
32. Wei Liu.; Dong duo Xu.; Xian Yue Dang.; Guo-Sheng Zhao.; Li-Min Chang.; Xin Li.; *Transaction of non ferrous metal society of China*.; **2015**., *25*, 1506-1516.
33. Azli,N. N. A.; Mohd Amin. N. F.; Oluhende, S. T.; Mohamad, S. N. A.; Fadil. M. A.; *Materials Today Proceedings*., **2021**, *39*, 1071-1076.